# Austral fall-winter transition of mesozooplankton assemblages and krill aggregations in an embayment west of the Antarctic Peninsula

Boris Espinasse, Meng Zhou, Yiwu Zhu, Elliott L. Hazen, Ari S. Friedlaender, Douglas P. Nowacek, Dezhang Chu, Francois Carlotti

Vol. 452: 63–80, 2012
doi: 10.3354/meps09626

MARINE ECOLOGY PROGRESS SERIES
Mar Ecol Prog Ser

Published April 25

# Austral fall–winter transition of mesozooplankton assemblages and krill aggregations in an embayment west of the Antarctic Peninsula

**Boris Espinasse[1], Meng Zhou[2,*], Yiwu Zhu[2], Elliott L. Hazen[3], Ari S. Friedlaender[3], Douglas P. Nowacek[3], Dezhang Chu[4], Francois Carlotti[1]**

[1]Laboratoire d'Océanographie Physique et Biogéochimique, Centre Océanologique de Marseille, CNRS, Université de la Méditerranée, Campus de Luminy, Case 901, 13288, Marseille Cedex 09, France

[2]Department of Environmental, Earth and Ocean Sciences, University of Massachusetts Boston, 100 Morrissey Boulevard, Boston, Massachusetts 02125, USA

[3]Nicholas School of the Environment and Pratt School of Engineering, Duke University Marine Laboratory, 135 Duke Marine Lab Road, Beaufort, North Carolina 28516, USA

[4]National Oceanic and Atmospheric Administration Fisheries, 2725 Montlake Boulevard E, Seattle, Washington 98112, USA

ABSTRACT: To assess krill aggregations and humpback whale *Megaptera novaeangliae* foraging behavior, spatial and temporal relationships between Antarctic krill *Euphausia superba* and zooplankton taxonomic groups were studied during an interdisciplinary cruise conducted in May and June 2009 within Wilhelmina Bay on the western side of the Antarctic Peninsula. A vessel-mounted acoustic Doppler current profiler (ADCP) and a calibrated EK-60 echo sounder were used to assess circulation patterns and krill distributions in the bay, and a multiple opening and closing net (with 333 µm mesh) and environmental sensing system (MOCNESS) was used to collect live samples of mesozooplankton and krill for taxonomic composition analysis. The results from this field study complement a previous one that examined an anticyclonic bay-scale circulation of Antarctic krill. This super-aggregation of krill covered ~100 km$^2$, had a concentration of 1000s of individuals m$^{-2}$ and was associated with more than 306 humpback whales present in Wilhelmina Bay. Our results from the mesozooplankton study revealed that krill continuously conducted diel vertical migrations and formed aggregations in the inner bay, while the chlorophyll concentration at the surface decreased from 2.2 to 0.6 g C m$^{-2}$ due to the decrease of daylight, and zooplankton concentrations increased from 0.5 to 1.5 g C m$^{-2}$ probably from advective influx. Most zooplankton were distributed below 200 m while krill fed in the upper 150 m. The spatial and temporal correlations between krill and small- to medium-sized mesozooplankton imply that krill may become omnivorous when there is a lack of phytoplankton in the late austral fall. Though both phytoplankton and zooplankton biomasses contributed only small fractions of the daily ration needed for krill metabolism in Wilhelmina Bay, it is not clear what caused krill to aggregate on such a large scale, as this led to high mortality as a result of starvation and predation by whales and other top predators.

KEY WORDS: Antarctic Peninsula · Chlorophyll · Zooplankton · Krill · Food web · Austral fall



## INTRODUCTION

Antarctic krill *Euphausia superba* plays a pivotal role in the Antarctic ecosystem linking primary producers to higher trophic level predators, such as penguins, seals and whales, and has been studied for more than 80 yr (Marr 1962, Laws 1985). Previous studies have significantly improved our understandings of their growth, seasonal behavior and life history (Quetin & Ross 1991, Huntley et al. 1994, El-Sayed

*Corresponding author. Email: meng.zhou@umb.edu

1996, Loeb et al. 1997, Everson 2000, Atkinson et al. 2002, Daly 2004, Siegel 2005, Tarling et al. 2006, Meyer et al. 2010). Adult krill are known to feed in regions on and off continental shelf breaks west of the Antarctic Peninsula during the summer, and then migrate inshore across the wide continental shelf during the fall and winter (Hofmann et al. 1988, Zhou et al. 1994, Lascara et al.1999, Ross & Quetin 2000, Siegel 2005). The krill overwintering strategies, which have been studied and demonstrated, include feeding on ice algae (Daly & Macaulay 1988, Marschall 1988), becoming omnivorous during this period (Price et al. 1988, Hopkins et al. 1993, Atkinson & Snÿder 1997, Zhou et al. 2004), reducing their metabolic rates (Quetin et al. 1994, Torres et al. 1994) and combusting their lipids, which sometimes results in shrinkage (Ikeda & Dixon 1982, Hagen et al. 1996). Feeding experiments and examinations of gut contents showed that *Euphausia superba* can feed on mesozooplankton and especially copepods (Price et al. 1988, Atkinson & Snÿder 1997). The relationships between Antarctic krill and prey may vary owing to the spatial and temporal variability of *in situ* plankton assemblages. The sea ice in coastal bays and shelf regions of the Antarctic Peninsula during the late fall and winter makes it difficult to sample krill and their prey fields (Hofmann et al. 2002). But prey–predator relationships are important for understanding krill overwintering strategies and the effects of climate change on the food web structure in the Southern Ocean.

The hydrography and circulation in the western Antarctic Peninsula (WAP) regions have been well documented (Hofmann et al. 1996, Smith et al. 1999, Zhou et al. 2002, 2006, Beardsley et al. 2004, Klinck et al. 2004). The main circulation patterns that affect this area are a northeastward current that transports the modified upper circumpolar deep water (UCDW) along the shelf break and intrudes onto shelf regions toward the tip of the Antarctic Peninsula, a southward baroclinic coastal current that is driven by freshwater runoff and the local gyres that are found over shelf basins and in coastal embayments. These physical processes are closely linked with biological processes in this region. Onshelf intrusions of the warm UCDW (>1°C) promote high primary productivity from November to March and are favorable for zooplankton growth (Rodriguez et al. 2002, Garibotti et al. 2003). Highest zooplankton abundances are typically found close to the coast (Hopkins 1985, Ashjian et al. 2004). Copepods widely dominate mesozooplankton biomass, and are one of major zooplankton taxa in the WAP regions (Ashjian et al. 2004, Ducklow et al. 2007). Adult *Euphausia superba* are found mainly around the inner shelf regions in the austral fall and winter. Both juvenile and adult krill are micronektonic and have strong swimming capabilities (Nicol 2003). They form dense aggregations as swarms or schools of various sizes (Zhou et al. 1994, Lawson et al. 2004, Zhou & Dorland 2004). Their swarming or schooling behavior has been thought to enhance their capability to forage or avoid predators (Hamner 1984, Zhou & Huntley 1996, Zhou & Dorland 2004).

Humpback whales *Megaptera novaeangliae* and minke whales *Balaenoptera acutorostrata* are commonly found in the WAP region where they feed preferentially on krill and fish (Thiele et al. 2004, Friedlaender et al. 2006, Nowacek et al. 2011). Late fall is a transition period for all the trophic levels in the WAP ecosystem when phytoplankton blooms end. Antarctic krill then migrate to the continental shelves and form aggregations in embayments where whales intensively feed on the krill before their seasonal migration or before overwintering. Large krill aggregations with a horizontal scale of more than 100s of meters and a concentration of more than 10s of individuals $m^{-2}$ have been frequently found in the WAP region (Zhou et al. 1994, Lawson et al. 2004, Zhou & Dorland 2004, Nowacek et al. 2011). The term superswarm of krill has been used to describe those aggregations that are up to several kilometers in size in the horizontal scale with a concentration of more than 100s of individuals $m^{-2}$ (Siegel & Kalinowski 1994). In this article, we use the term of aggregation instead of swarm or school because of difficulties separating *in situ* swarms and schools.

An interdisciplinary cruise was conducted in late austral fall 2009 within the WAP embayments to study krill aggregation and humpback whale fine-scale foraging behavior, and predator–prey ecology. During the cruise, super-aggregations of Antarctic krill and humpback whales were found in Wilhelmina Bay (Nowacek et al. 2011). During the month-long cruise, the concentration of chlorophyll *a* (chl *a*) decreased from 1.5 µg chl *a* $l^{-1}$ to nearly zero, which indicated the end of the productive season. Under such a physical and biological setting, this article examines the results from the analysis of mesozooplankton and krill live samples for spatial and temporal distributions and their relationships. Krill food demands, grazing effects on zooplankton community structures and evolution of the zooplankton and krill abundances and size spectra were inferred from these relationships and from values obtained from the literature for assessing the overwinter strategy used by krill of forming a super-aggregation to feed on zooplankton.

## MATERIALS AND METHODS

### Study sites

Our study focused on the Gerlache Strait and its embayments in the Antarctic Peninsula (Fig. 1). The southern end of the strait is ~100 m deep and opens to the Bismarck Strait, which is over 200 m deep and linked to deep canyons on the shelf. The northern end is ~600 m deep and opens to the western Bransfield Strait. Wilhelmina Bay is an embayment within the Gerlache Strait and has an area of ~600 km$^2$. The mean depth of the deep channel in the Wilhelmina Bay is ~300 m while the deepest depth is over 600 m. These deep channels on the shelf of the WAP allow the UCDW to intrude onto the shelf regions and coastal embayments, which is critically important to ecosystem processes in the WAP (Hofmann et al. 1996).

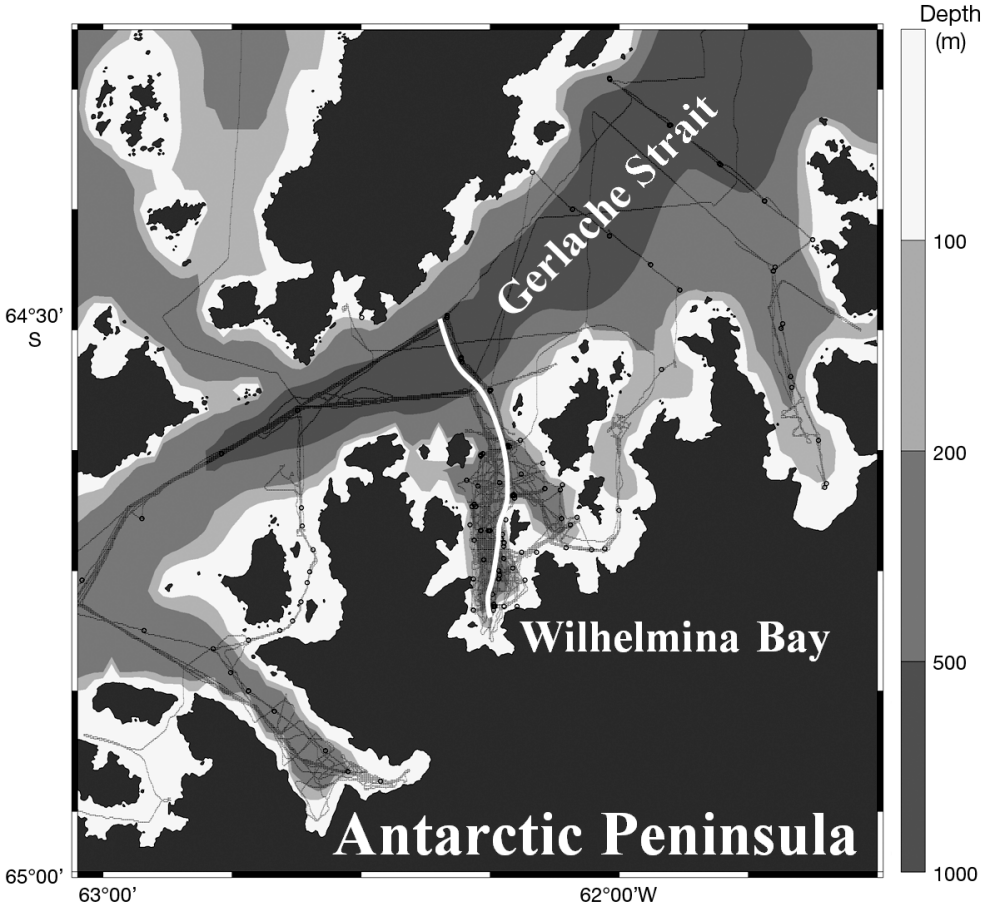


Fig. 1. Bathymetry of Wilhelmina Bay and its vicinity. The gray color scale represents the bathymetry, black dots were CTD stations, black lines represent ADCP surveys and the white line represents the transect shown in Fig. 3

### Data collection and sampling

Cruises were conducted onboard the Antarctic Service and Research Vessel (ASRV) 'LM Gould' from April 21 to June 11, 2009, on 3 separate occasions, or legs: May 1 to 9, May 16 to 22 and May 26 to June 3. During each leg, hydrography, currents, krill and zooplankton were measured: currents and acoustic volume backscattering were measured with a vessel-mounted, narrow band, 153 kHz acoustic Doppler current profiler (ADCP; RD Instruments); hydrography was measured with a CTD (Sea-Bird 911 plus, Sea-Bird Electronics); fluorescence, as an index of chl *a* concentration, was measured with an ECO-AFL/FL fluorometer (WET Lab); zooplankton were collected and measured for size and taxonomic composition by means of a 1 m$^2$ multiple opening and closing net (333 µm mesh) and environmental sensing system (MOCNESS; Wiebe et al. 1976, 1985) . In Wilhelmina Bay, 35, 15 and 24 CTD stations were conducted during Legs 1, 2 and 3, respectively, and all 3 paired MOCNESS tows were conducted within and outside of krill aggregations at night.

Before the cruise all CTD sensors were calibrated within standard initial accuracies of 0.001°C for temperature and 0.003 mmho cm$^{-1}$ for conductivity. The differences between the pair of CTD sensors were the same as the initial accuracies during the cruise. All CTD data were first processed by applying filters and corrections as suggested by Sea-Bird Electronics, and then were binned to 1 m depth intervals. The 95% CIs for the mean temperature and salinity in a 1 m bin are less than 0.003°C and 0.003, respectively. The ECO-AFL/FL fluorometer was integrated with the CTD.

The ADCP was configured for both current and volume backscattering measurements. Both the pulse and bin lengths were set at 8 m, and blank (i.e. set to not receiving signals) after transmission was set to 4 m. A 5 min ensemble average was

made for the current measurements with a 95% CI of 1.1 cm $s^{-1}$ (RDI 1989). The tidal currents were estimated with the model developed by Padman et al. (2002) and removed from the ADCP current measurements. To further eliminate inertial oscillation, the detided ADCP currents were fitted with a streamfunction during objective analysis (Bretherton et al. 1976, Dorland & Zhou 2008).

The ADCP provided echo intensity measurements with an accuracy of 1 dB for a single ping but was not calibrated. An echo sounder (Simrad EK-60, 120 kHz, Kongsberg-Simrad) was used on a zodiac inflatable boat for mapping the fine scale of krill aggregations around a feeding whale and was calibrated by using a standard 3 cm tungsten–carbide sphere following standard procedures (Foote et al. 1990). To correct ADCP biomass concentration estimates that used the calibrated EK-60, a calibration experiment was done at Stn B during which the zodiac with the EK-60 sailed ~50 m ahead of the ARSV 'LM Gould' at 2 knots for ~35 min between 18:49 h and 19:24 h local time on May 8, 2009. To compare ADCP and EK-60 backscattering data, both data sets were averaged over 30 min during data processing for removing potential errors due to fine-scale krill aggregations and differences in the beam patterns between the EK-60 and ADCP. The krill target strengths were estimated based on the mean and SD of krill length analyzed from MOCNESS samples, literature values on the orientations, material properties and the deformed cylinder model (Chu et al. 1993, Chu & Wiebe 2005, Lawson et al. 2006). Both EK-60 and ADCP volume backscattering data (in dB) were converted to biomass wet weight (WW) concentrations of krill (in g $m^{-3}$) by using a prolate spheroid model and the density of an individual krill of ~1 g WW $cm^{-3}$. To correct the ADCP estimates, the constants for the power into water ($K_2$) and automatic gain control ($K_c$) in the ADCP sonar equation are corrected for the acoustic energy loss and ship noise by least squares fitting, which minimized the difference between EK-60 and ADCP biomass estimates (Flagg & Smith 1989, RDI 1989, Zhou et al. 1994). After such an empirical calibration, the ADCP volume backscattering data were used to estimate krill biomass.

The ADCP acquired volume backscattering data continuously during the entire cruise. The daytime activities for spatial surveys of whales and following tagged whales with a satellite transmitter provided some ADCP coverage in Wilhelmina Bay while nighttime activities such as ADCP mapping and hydrographic surveys provided the coverage of acoustic backscattering data in the entire Wilhelmina Bay. The EK-60 was only operated during the day under fair weather conditions. Most of time, the zodiac was working around the vicinity of a tagged whale while the ASRV 'LM Gould' was elsewhere conducting spatial surveys of whales. They only ran in parallel when conducting the calibration.

Zooplankton samples were collected by the MOCNESS at 2 stations in all 3 legs (Fig. 1). One sampling station was located within the krill aggregations, and another was located outside of the aggregations for comparative purposes. Before or after each net tow, a CTD–fluorometer (CTDF) cast was conducted at the net tow station. To be consistent, all MOCNESS tows for sampling krill and zooplankton were conducted at night when krill were distributed in the upper water column (Table 1). Whale observations, tagging and tracking typically took place during the day. The depth interval for each net was chosen by using the information on krill vertical distributions that was provided in real time by the biomass estimates from processed ADCP backscattering data. Some depth intervals were merged to make data comparable between ADCP and net tows resulting in 6 and 7 depth layers defined at Stns A and B, respectively.

All live samples were immediately preserved in 5 to 10% buffered formalin in seawater after collection. When the entire sample in a net was too large to be preserved, the sample was split and a subsample was preserved for future analysis. During the post labora-

Table 1. Geographic locations, bottom depths, dates and times of MOCNESS tows

| Station | Latitude (S) | Longitude (W) | Bottom depth (m) | Tow depth (m) | Leg | Date (d/mo/yr) | Time (h) |
|---|---|---|---|---|---|---|---|
| Stn A | 64° 36′ | 62° 15′ | 380 | 350 | 1 | 06/05/2009 | 03:20 |
| (low krill concentration) | | | | | 2 | 18/05/2009 | 22:30 |
| | | | | | 3 | 30/05/2009 | 04:50 |
| Stn B | 64° 40′ | 62° 15.5′ | 600 | 500 | 1 | 02/05/2009 | 02:10 |
| (high krill concentration) | | | | | 2 | 18/05/2009 | 20:10 |
| | | | | | 3 | 30/05/2009 | 02:30 |

tory analysis, a 6 mm mesh filter was used to separate mesozooplankton and adult krill. The samples were thoroughly rinsed to ensure all the mesozooplankton passed through the filter. Some samples were further divided with a Motoda splitter resulting in a subsample with no fewer than 1000 individuals.

### Data analysis

An aliquot of each sample with organisms less than 6 mm was processed by using ZOOSCAN (www.zooscan.com). Each scanned image had a resolution of 2400 dots per inch (dpi) and were analyzed with the software Zooprocess (Grosjean et al. 2004), which is embedded in the image analysis software ImageJ (Rasband 2005). A total of 46 variables, including geometrical and optical characteristics, were measured by Zooprocess for each individual and then used by the software Plankton Identifier for automated classification based on the supervised learning algorithms implemented in free statistical pack TANAGRA (Rakotomalala 2005, Gasparini 2007). Six predefined categories (e.g. copepods, chaetognaths, a group consisting of ostracods, polychaetes and pteropods, krill larvae, krill appendages and detritus) were chosen based on their dominances and identifiable features. The automatic classification is based on the random forest algorithm that used the 46 variables analyzed by Zooprocess (Breiman 2001). Finally, a manual verification was done by comparing random selected images and taxonomic identifications to ensure the quality of automated zooplankton analysis.

We performed a microscopic analysis to establish the copepod categories. Four groups of copepods based on total length were defined: small copepods <1.4 mm, small to medium copepods 1.4–2.8 mm, medium to large copepods 2.8–4.1 mm and large copepods >4.1 mm. These size ranges comprise the following: small copepods are dominated by *Oithona* spp., *Oncaea* spp. and *Microcalanus pygmaeus*; small to medium copepods are dominated by copepodite stages III, IV and V of *Metridia gerlachei*; medium to large copepods are dominated by adult *Metridia gerlachei*; and large copepods primarily consist of 4 calanoid species — *Calanus acutus*, *C. propinquus*, *Euchaeta antarctica* and *Rhincalanus gigas*.

The formula used for converting the area measured by the software Zooprocess to biovolume (BioV) is

$$\mathrm{BioV} = \frac{4}{3} \times \frac{\mathrm{Area}}{\sqrt{\mathrm{Ratio}}} \times \sqrt{\frac{\mathrm{Area}}{\pi}} \quad (1)$$

where Ratio is the ratio between the major and minor axes of the prolate spheroid corresponding to the body of an individual measured manually for copepods. We assumed the ratios of 8 and 20 for krill and chaetognaths, respectively, to convert an image area to the biovolume. To convert biovolume to biomass in WW, the density of 1 mg WW $mm^{-3}$ is used for zooplankton and krill (Wiebe et al. 1975).

## RESULTS

The seasonal cooling process in Wilhelmina Bay was observed but weak (Fig. 2). The temperature at the surface varied between −0.6 and −0.9°C during Leg 1, −0.5 and −0.6°C in Leg 2 and −0.2 to −0.7°C in Leg 3 (Fig. 2). Chlorophyll concentrations reached 0.9 and 1.5 mg $m^{-3}$ during Leg 1 at Stns A and B, respectively. It decreased to <0.25 mg $m^{-3}$ during Legs 2 and 3 at both Stns A and B. Details of the hydrographic conditions are shown on the transect along the north–south major axis of Wilhelmina Bay in Leg 3 (Fig. 3). The lowest temperature occurred at the surface of the inner bay while the highest temperature occurred at the depth near the Gerlache Strait. The salinity at the surface in the inner bay was the lowest while the halocline was uplifted toward the inner bay. The streamfunction-fitted cur-

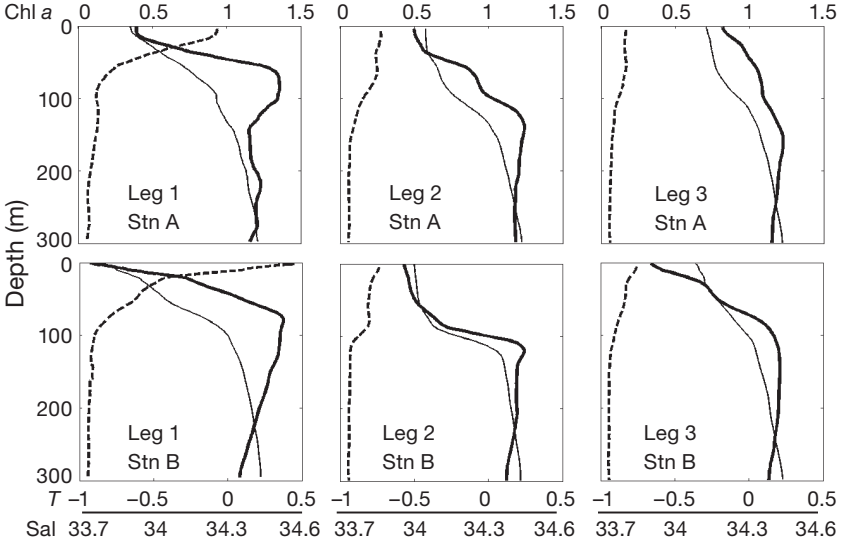


Fig. 2. Vertical profiles of temperature (*T*, °C) (thick solid lines), salinity (Sal, thin solid lines) and chl *a* (mg $m^{-3}$) (dashed lines) at Stns A and B during 3 legs

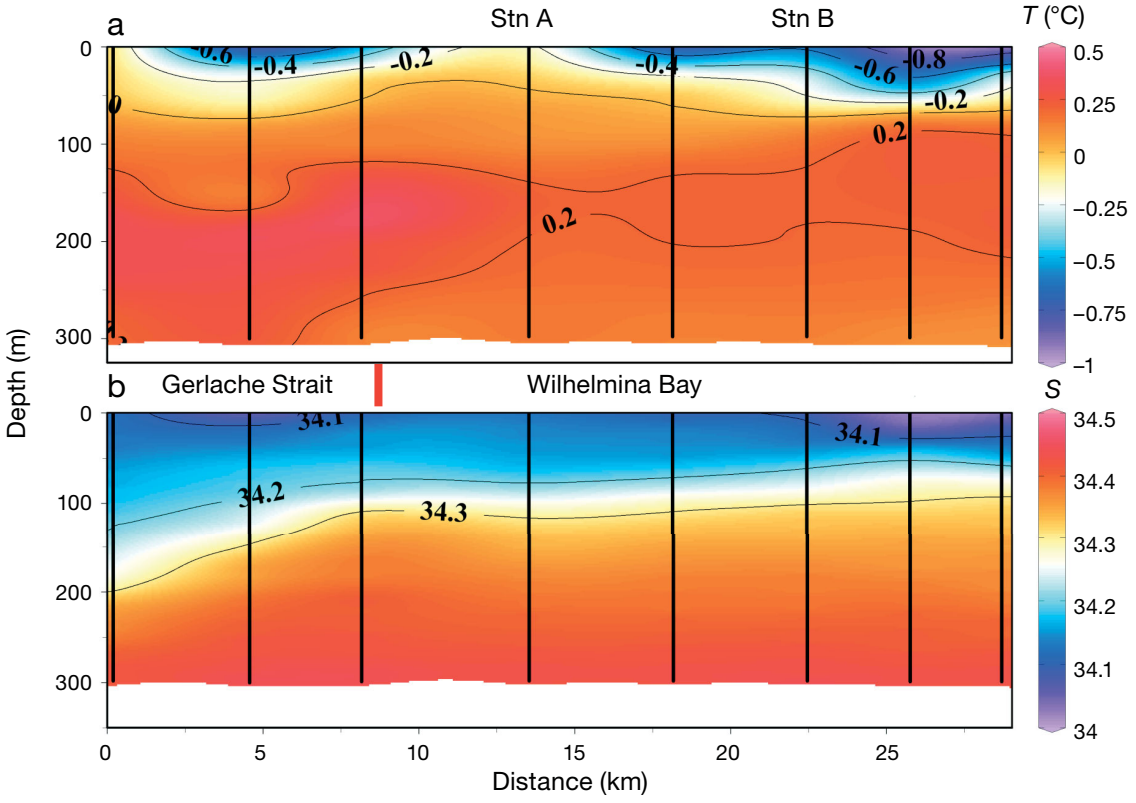


Fig. 3. (a) Temperature ($T$) and (b) salinity ($S$) transects from the Gerlache Strait to the inner Wilhelmina Bay during Leg 3 (transect location indicated in Fig. 4). The vertical black lines correspond to CTD stations

rent field at 22 m showed an anticyclonic eddy along the isobaths of the deep basin occupying most of Wilhelmina Bay (Fig. 4).

The results from krill length–frequency distributions of MOCNESS samples are shown in Fig. 5, resulting in a mean (±SD) length of 42 ± 6 mm and a length to height ratio of 8. Applying the measured mean (±SD) length as well as the krill mean (±SD) orientation of 4 ± 14° and krill material properties, both obtained from literature, and the acoustic deformed cylinder model (Chu et al. 1993, Chu & Wiebe 2005, Lawson et al. 2006), we calculated that the mean krill target strengths were −72 and −75 dB for 120 and 153 kHz, respectively. Both EK-60 and ADCP volume backscattering measurements were converted to biomass concentration of krill (g WW $m^{-3}$). The results from the linear regression between EK-60 and ADCP estimated biomass are shown in Fig. 6 ($y$ = 0.9603$x$ + 0.506 and $r^2$ = 0.91). This regression relationship is applied to correct all ADCP biomass estimates in Wilhelmina Bay where the calibration between EK-60 and ADCP was done.

A super-aggregation of krill with a horizontal area of ~10 × 10 $km^2$ and vertical layer thickness of ~250 m was found by using the ADCP acoustic mapping at night in Wilhelmina Bay between May 1 and 3, 2009 (Fig. 7). This aggregation remained in the bay during our study period and was foraged by the high density of humpback whales (Nowacek et al. 2011). The super-aggregation had a mean density of 130 g WW $m^{-3}$ and a maximum density of 1500 g WW $m^{-3}$, corresponding to 170 and 2000 individuals (ind.) $m^{-3}$, respectively. Our estimate of total krill biomass in this super-aggregation based on the ADCP data corrected by using the calibrated EK-60 over the entire survey area in Wilhelmina Bay was 2.3 million t in Leg 1. By using the 120 kHz EK-60 data collected in daytime, we found the overall mean density was 62 g WW $m^{-3}$ during the daytime, which was less than the estimate of 130 g WW $m^{-3}$ made by ADCP mostly during the nighttime. Such a difference in 153 kHz ADCP and 120 kHz EK-60 biomass estimates could be explained by diel vertical migration of krill that was observed during the entire cruise (Fig. 8).

The mean (±SD) length–height aspect ratios of copepods from manually analyzed prosome length and width are 2.85 ± 0.25 (n = 29), 3.08 ± 0.30 (n = 28), 2.92 ± 0.18 (n = 25) and 3.69 ± 0.52 (n = 19) for small, small to medium, medium to large and large copepods, respectively. Using these aspect ratios for cope-

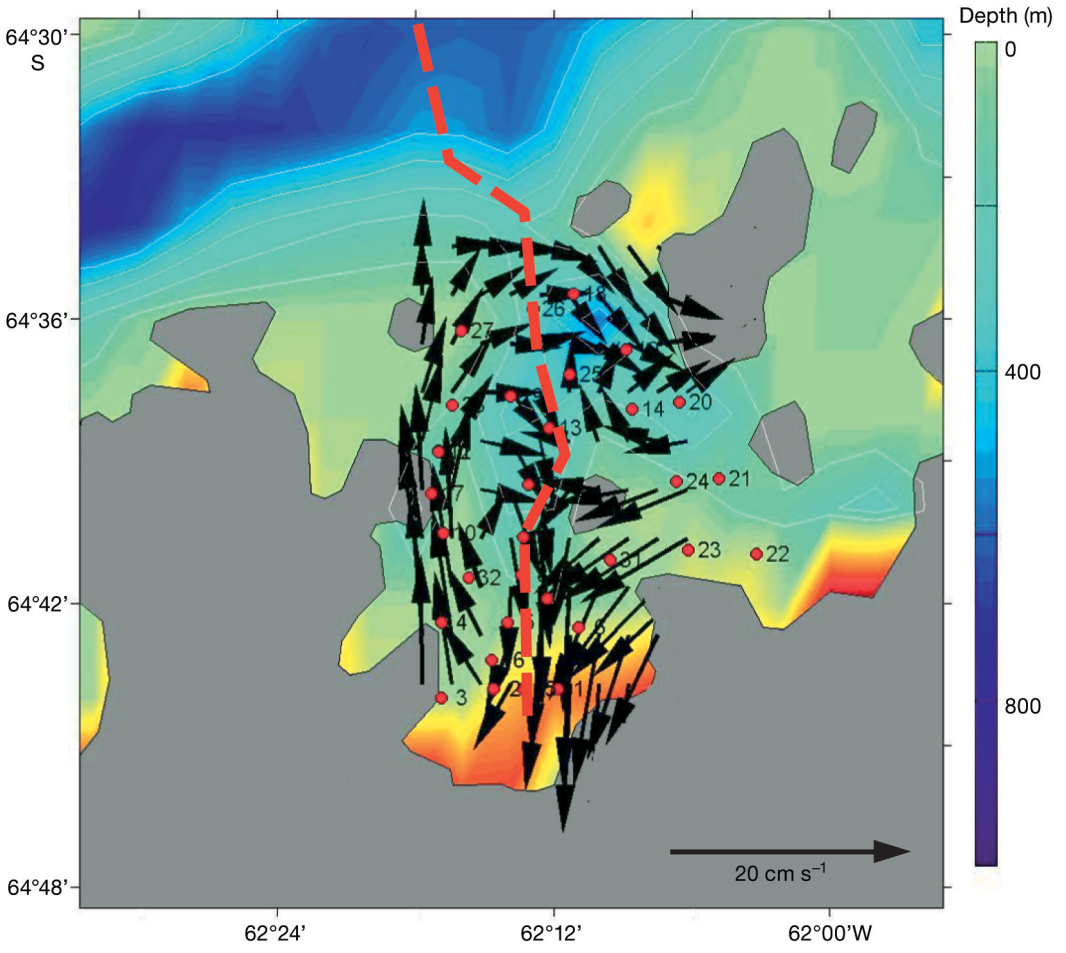


Fig. 4. Current field at 22 m inferred from the objective streamfunction fitting to the acoustic Doppler current profiler current measurements. The black arrows represent the current at 22 m, the thick red dashed line represents the transect shown in Fig. 3, the false colors represent the isobaths and the red dots represent CTD stations

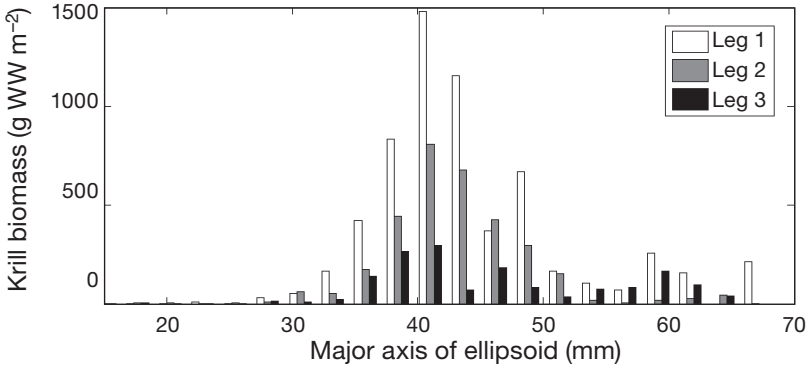


Fig. 5. *Euphausia superba*. Size–biomass histogram of krill (g wet weight [WW] m$^{-2}$). The length interval is 2 mm

pods, 8 for krill and 20 for chaetognaths, and assuming a ratio of 0.12 mg C per mg WW for both copepods and euphausiids and 0.03 mg C per mg WW for chaetognaths (Harris et al. 2000), the depth-integrated WW and carbon biomasses for phytoplankton, copepods, krill and chaetognaths at the 2 sampling stations for all 3 cruises are shown in Table 2. To estimate carbon biomass for phytoplankton, we assumed a ratio of 50:1 of C to chl *a* in weight (Mitchell & Holm-Hansen 1991). Because the fluorometer used was not calibrated, a carbon biomass estimate for phytoplankton can be used only as an index. Whereas the phytoplankton biomass values at both stations were similar and declined monotonically from Leg 1 to Leg 3, copepods biomass was ~2 to 3 times higher at Stn B than at Stn A during all 3 legs. The small copepod size class dominated the abundance at Stn A and the small to medium and medium to large size groups dominated the abundance at Stn B during all 3 legs (Table 3). For the biomass, the small to medium and medium to large groups were dominant at Stn A while the medium to large group was dominant at Stn B.

Krill biomass estimates were ~30 times higher at Stn B than at Stn A during Legs 1 and 2 and decreased by ~10 times during Leg 3 (Table 2). The

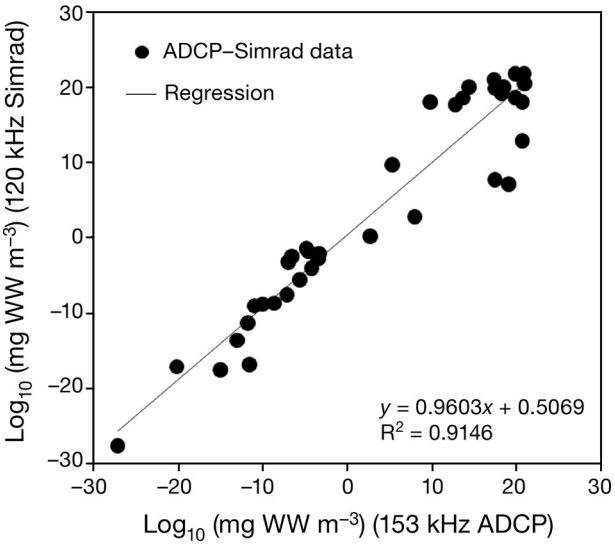


Fig. 6. *Euphausia superba*. Scatter plots between the corrected acoustic Doppler current profiler (ADCP) and calibrated echo sounder EK-60 krill biomass concentrations estimated from the calibration experiment conducted at Stn B. The data were 30 min averaged for removing small-scale spatial variability in zooplankton and krill distributions. In the experiment, the zodiac with the EK-60 was 50 m ahead of the ARSV 'LM Gould', and both moved at 2 knots on the same straight line for ~30 min in the evening on May 8, 2009. WW: wet weight

krill biomass decreased by a factor of 4 from Leg 1 to Leg 3 at Stn B while the low krill biomass remained at Stn A during the study period. Inversely, from Leg 1 to Leg 3, the copepod biomass increased by 3 times at Stn B while it increased only slightly at Stn A. The chaetognath biomass remained at similar level between Stns A and B while larger fluctuations occurred at Stn B than at Stn A.

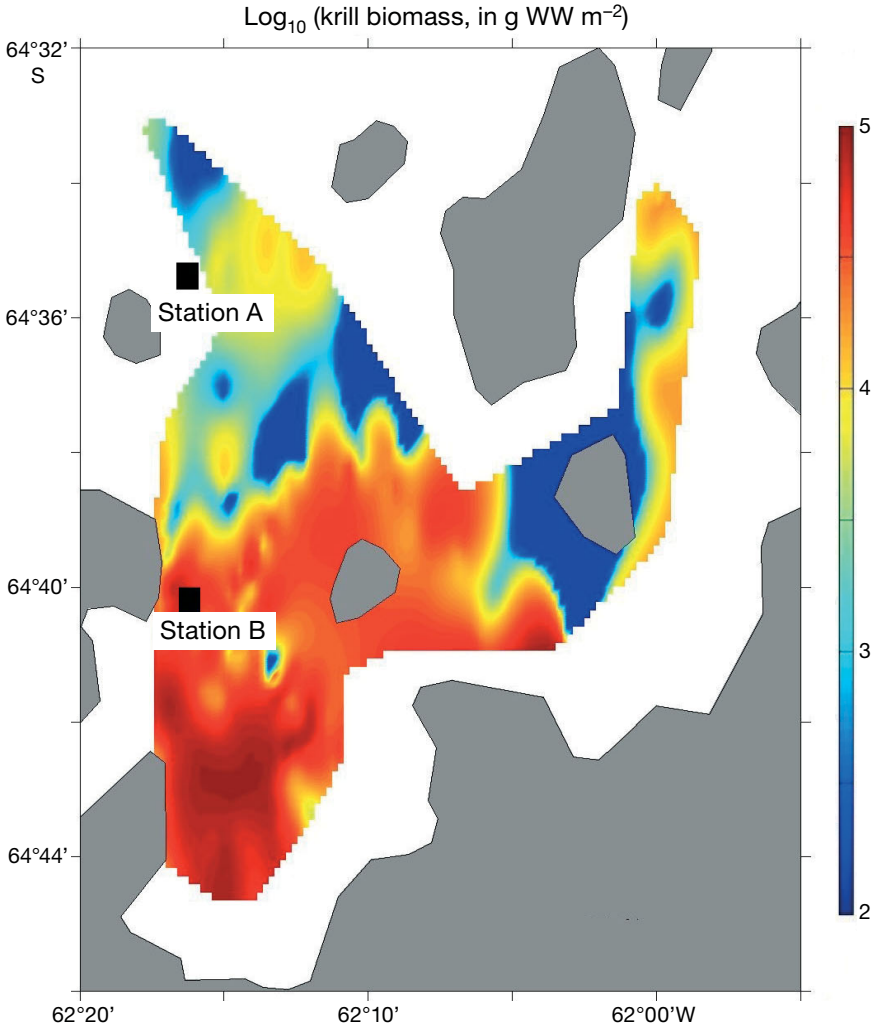


Fig. 7. *Euphausia superba*. Krill biomass distribution (g wet weight [WW] $m^{-2}$) estimated from corrected backscattering measurements performed with an acoustic Doppler current profiler between May 1 and 3, 2009, during Leg 1. (■): locations of Stns A and B

The vertical distribution patterns in krill biomass were similar at Stns A and B for all 3 legs though the biomass at Stn A was significantly lower than at Stn B (Fig. 9). Krill aggregations ranged from 0 to 350 m during Leg 1, and from 0 to 150 m during Legs 2 and 3. Chaetognaths and large copepods dominated the biomass distribution at Stn A below 150 m while small to medium and medium to large copepods (primarily *Metridia gerlachei*) dominated the upper 150 m (Fig. 10). At Stn B, the medium to large group dominated the biomass below 350 m. The biomass values in the upper 150 m were 74, 76 and 64%, which were significantly less than those at Stn A in Legs 1, 2 and 3, respectively. During Leg 3 at Stn A, the maximum biomass concentrations of small to medium and medium to large copepods were found between 50 and 100 m while their minimum concentration occurred below 150 m, and the maximum concentrations of chaetognaths and large copepods were below 150 m. At Stn B, the minimum biomass concentrations of small to medium and medium to large copepods were found in the upper

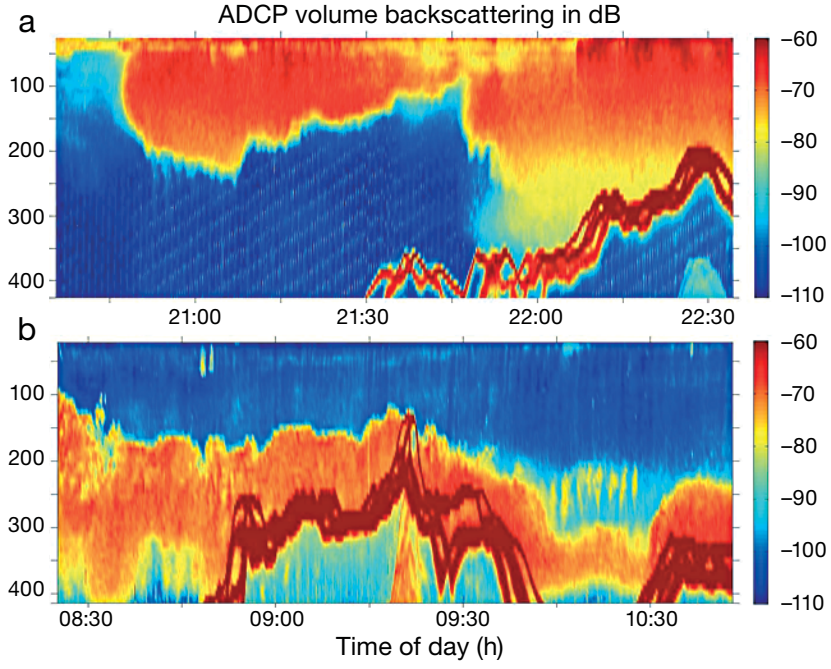


Fig. 8. Acoustic Doppler current profiler (ADCP) backscattering measurements (dB) (a) during the night on May 1, 2009 and (b) during the day on May 3, 2009 at Stn B

150 m and increased monotonically in the depth below 150 m.

The small copepods were most abundant and were followed by small to medium copepods at Stn A where krill aggregations were absent (Fig. 11). Conversely, the small and small to medium copepods were least abundant in the upper 100 to 150 m at Stn B. The small to medium and medium to large groups increased in abundance with depth, and were most abundant below 350 m. The ADCP measurements of krill biomass and depth ranges at Stn B corresponded negatively to copepod abundances and biomasses (Fig. 11).

A principal component analysis (PCA) on zooplankton taxonomic groups and krill abundances was conducted for all the samples collected at Stn B in order to identify the interactions between the krill and zooplankton taxonomic groups at different depth layers. Unidentifiable taxa belonging to the group 'others' were not included in this analysis. The first 2 components accounted for 85.9% of the entire variability (Table 4). The first mode showed a strong negative correlation between krill abundance and all zooplankton groups, particularly the small and small to medium copepods. No significant pattern was associated with the second mode of variability. The correlation circle formed by PC1 and PC2 shows the strongest negative correlations among small and small to medium copepods and krill with difference in angles of nearly 180°, which suggests either a predator–prey interaction is present or that they are not distributed in same regions (Fig. 12). The angles between medium to large copepods (primarily *Metridia gerlachei*), chaetognaths and krill

Table 2. Biomasses in wet weight (g WW $m^{-2}$) and carbon content (g C $m^{-2}$) of plankton taxonomic groups in specified sampling depth ranges based on live samples collected using the MOCNESS during 3 legs at Stns A and B. Sample depth was 350 m at Stn A and 500 m at Stn B

| Taxonomic group | Leg 1 | | Leg 2 | | Leg 3 | |
|---|---|---|---|---|---|---|
| | WW | Carbon | WW | Carbon | WW | Carbon |
| **Stn A** | | | | | | |
| Phytoplankton (chl *a*)[a] | 0.046 | 2.3 | 0.022 | 1.1 | 0.013 | 0.69 |
| Copepods[b] | 1.83 | 0.21 | 3.04 | 0.36 | 3.44 | 0.41 |
| Krill[b] | 198 | 23.7 | 88 | 10.5 | 167 | 20.0 |
| Chaetognaths[b] | 1.92 | 0.05 | 1.78 | 0.05 | 1.24 | 0.03 |
| **Stn B** | | | | | | |
| Phytoplankton (chl *a*) | 0.043 | 2.15 | 0.017 | 0.88 | 0.012 | 0.62 |
| Copepods | 4.57 | 0.54 | 5.77 | 0.69 | 12.5 | 1.50 |
| Krill | 6657 | 798 | 2987 | 358 | 1730 | 207 |
| Chaetognaths | 0.56 | 0.01 | 2.58 | 0.07 | 1.64 | 0.04 |

[a]A carbon to chl *a* ratio of 50 was used (Mitchell & Holm-Hansen 1991)
[b]Carbon to WW ratios of 0.12, 0.12 and 0.03 were used for copepods, euphausiids and chaetognaths, respectively (Harris et al. 2000)

Table 3. Abundance and biomass proportions (means ± SD) of zooplankton per size categories (small <1.4, small to medium 1.4–2.8 mm, medium to large 2.8–4.1 mm, large >4.1 mm) at Stns A and B based on all live samples collected using the MOCNESS during all 3 legs

| Zooplankton group | Abundance (%) | | Biomass (%) | |
|---|---|---|---|---|
| | Stn A | Stn B | Stn A | Stn B |
| Small copepods | 56.7 ± 7.8 | 24.3 ± 1.1 | 5.7 ± 1.7 | 1.6 ± 0.1 |
| Small to medium copepods | 28.4 ± 6.6 | 34.4 ± 7.0 | 15.8 ± 8.0 | 11.4 ± 2.8 |
| Medium to large copepods | 5.6 ± 2.5 | 31.5 ± 6.6 | 16.3 ± 7.7 | 45.3 ± 11.2 |
| Large copepods | 1.0 ± 0.3 | 2.2 ± 0.7 | 15.7 ± 1.0 | 16.7 ± 5.6 |
| Chaetognaths | 5.6 ± 3.8 | 4.7 ± 3.1 | 32.4 ± 8.2 | 16.0 ± 9.6 |
| Others | 2.4 ± 1.2 | 2.5 ± 1.2 | 13.9 ± 5.8 | 8.8 ± 2.9 |

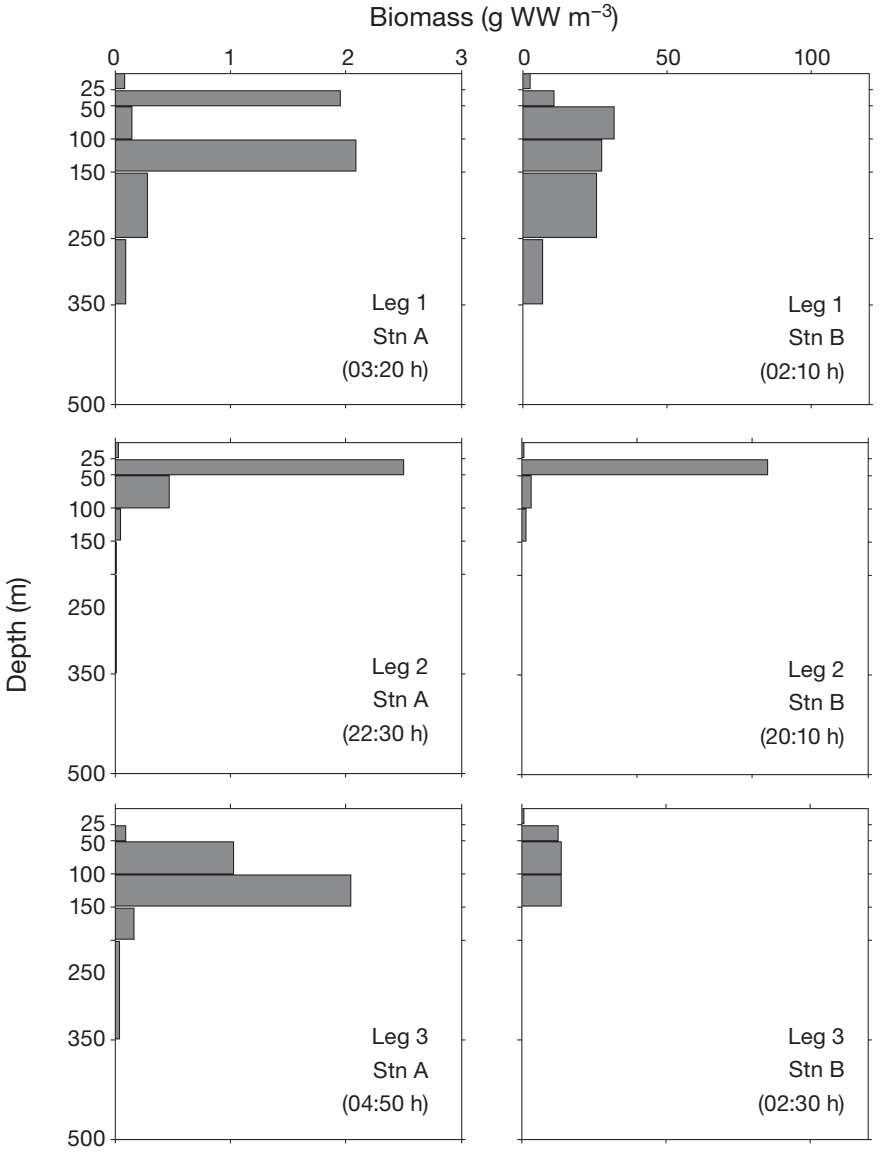


Fig. 9. *Euphausia superba*. Vertical profiles of krill biomass (g wet weight [WW] m$^{-3}$) at Stns A and B during 3 legs

are smaller, which means there is a less dependent distribution pattern among these 3 taxonomic groups.

## DISCUSSION

### Hydrography and circulation

The water characteristics of the deep water found in Wilhelmina Bay were the same as the modified UCDW found in the Gerlache Strait (Niiler et al. 1991, Hofmann et al. 1996). The temperature reached 0.3°C in both the inner and outer parts of the bay (Figs. 2 & 3). The horizontal temperature gradient showed a greater concentration of heat at the Gerlache Strait. The upward tilted thermocline and halocline towards the inner bay implied there was an upwelling in the inner bay. The northward dominant katabatic wind occurred frequently during the survey period and drove a clockwise gyre around the deep basin in Wilhelmina Bay, which consisted of a surface northward outflow at the western side of the bay, an upwelling at the inner bay and a southward re-circulation at the eastern side of the bay (Fig. 4). To compensate for the surface outflow and upwelling at the inner bay, a deep southward compensation current was identified from the warm temperature in the deep water that originated from the modified UCDW in the Gerlache Strait. The upwelling driven by katabatic winds convected the warm deep water to the upper layer and kept the bay from freezing, a condition that was critical in allowing air-breathing predators such as whales, seals and penguins to access to krill.

The circulation in Wilhelmina Bay can also be affected by the potential vorticity conservation

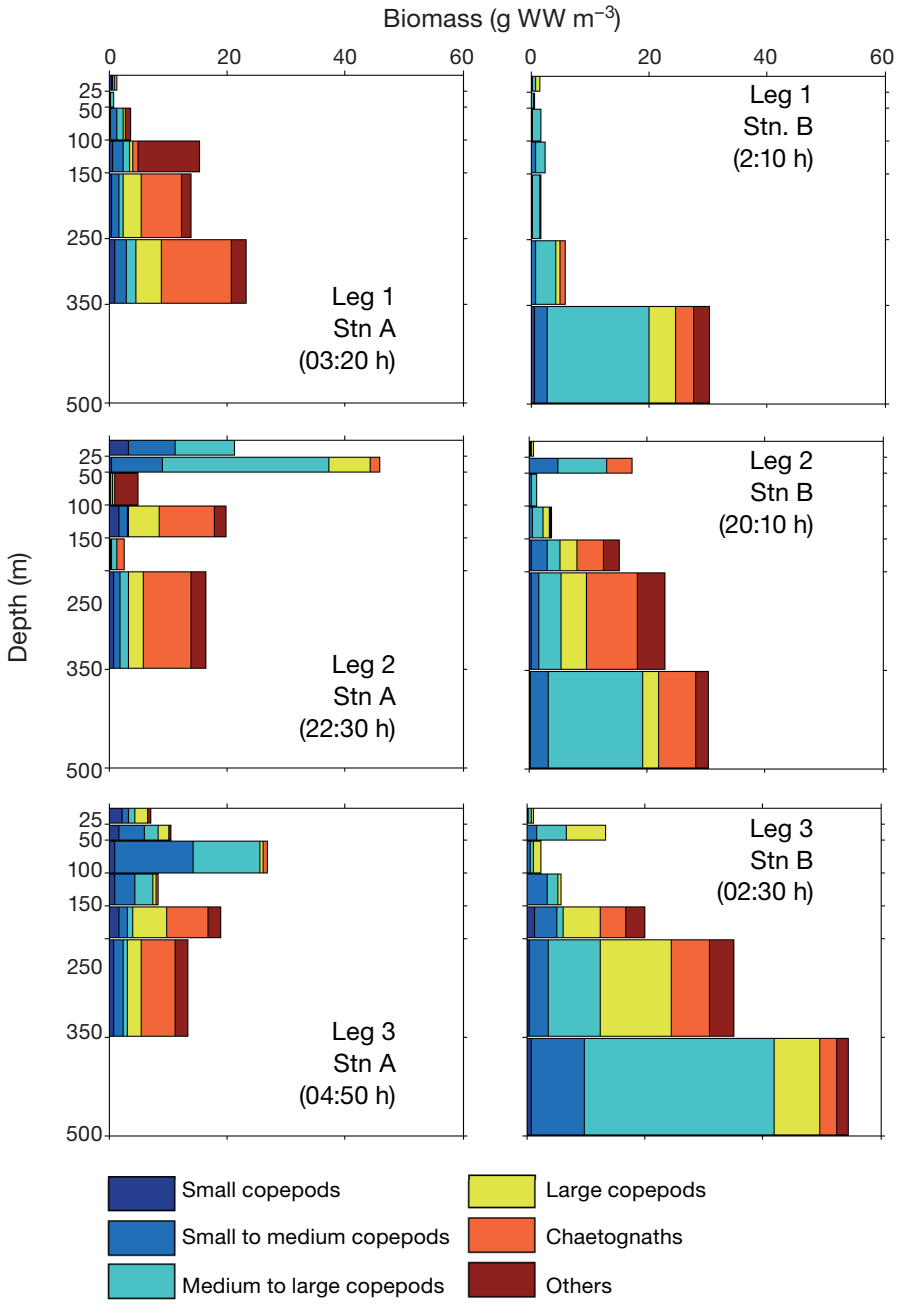


Fig. 10. Vertical profiles of zooplankton biomass (g wet weight [WW] m$^{-3}$) in size classes (see Table 3) at Stns A and B

(Pedlosky 1987). The clockwise surface circulation along isobaths implies that the barotropic nature of the circulation in the bay penetrated into the whole water column, and was controlled by the topography (Fig. 4). Because the current followed the isobaths, the deep channel between Wilhelmina Bay and the Gerlache Strait allowed the water to exchange, which allowed warmer Gerlache Strait waters to replace cooler Wilhelmina Bay waters. Thus, a deep channel that allows deep water intrusions in a bay or fjord at high latitudes is a critical physical process that provides heat flux and biota in deep waters for krill and fall–winter habitat for top predators.

### Krill size and biomass distributions

The krill mean length ± SD obtained from the size distribution of krill analyzed from MOCNESS samples was 42 ± 6 mm. There were very few krill <20 mm or >60 mm during all 3 legs (Fig. 5). The abundance of krill decreased from Leg 1 to Leg 3. The peak sizes and the shapes of length frequency distributions were not significantly changed across these 3 legs, which implies that mortality or emigration from the area of study was uniform across all krill size classes. If starvation and predation by whales or other krill predators contributed to krill mortality, then the overall effect on krill size distributions were not size-specific.

The estimate of total krill biomass in Wilhelmina Bay was ~2.3 million t (WW) determined from calibrated ADCP backscattering measurements during Leg 1. It is well known that ADCP absolute backscattering measurements are problematic (Flagg & Smith 1989, Zhou et al. 1994). Brierley et al. (1998), using an ADCP at 153 kHz, showed that the krill biomass estimates in a depth shallower than ~150 m were comparable in magnitude to those determined with an EK-60 at 120 kHz, while the ADCP estimates in a depth deeper than 150 m were 1 to 2 orders of magnitude less than those determined with an EK-60. The difference increased as a function of depth. The difference was here empirically corrected by using a depth-varying gain, $k_c$, which significantly improved the linear regression between ADCP and EK-60 krill biomass estimates (Fig. 6). Because the $k_c$

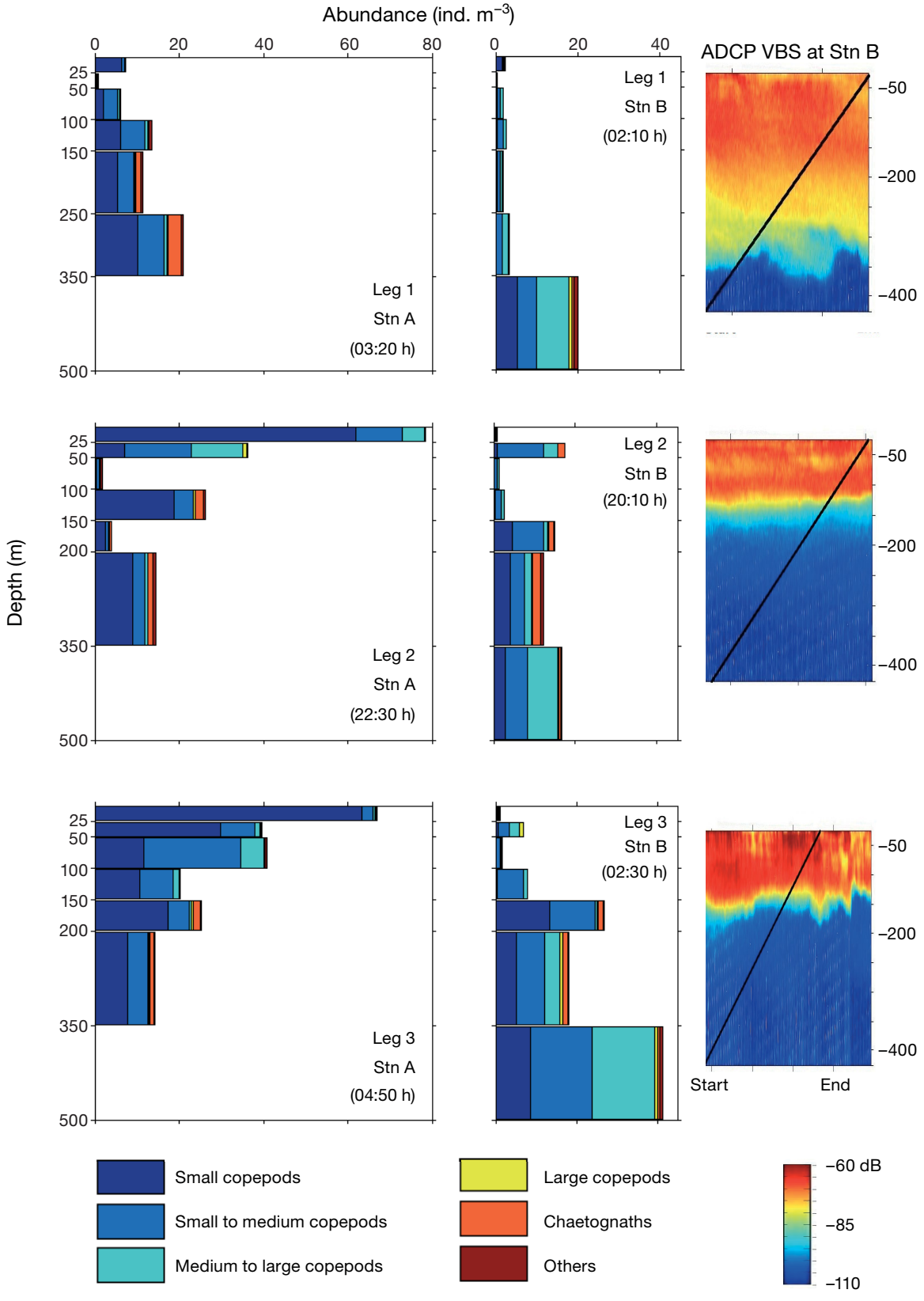


Fig. 11. Vertical profiles of zooplankton abundance (ind. m$^{-3}$) within size classes (see Table 3) at Stns A and B and acoustic volume backscattering (VBS, in dB) at Stn B collected during net tows using an acoustic Doppler current profiler (ADCP). The black lines represent the approximate upcasting trajectories of the MOCNESS tows

Table 4. Correlation coefficients and percentages of the total variance (in parentheses) associated with the first 2 principal components of zooplankton size groups (see Table 3) based on live samples collected using the MOCNESS

| Zooplankton group | PC1 (70.4 %) | PC2 (15.5 %) |
|---|---|---|
| Small copepods | −0.89 | 0.27 |
| Small to medium copepods | −0.91 | 0.11 |
| Medium to large copepods | −0.70 | −0.62 |
| Large copepods | −0.77 | −0.37 |
| Chaetognaths | −0.72 | 0.55 |
| Krill | 0.99 | 0.02 |

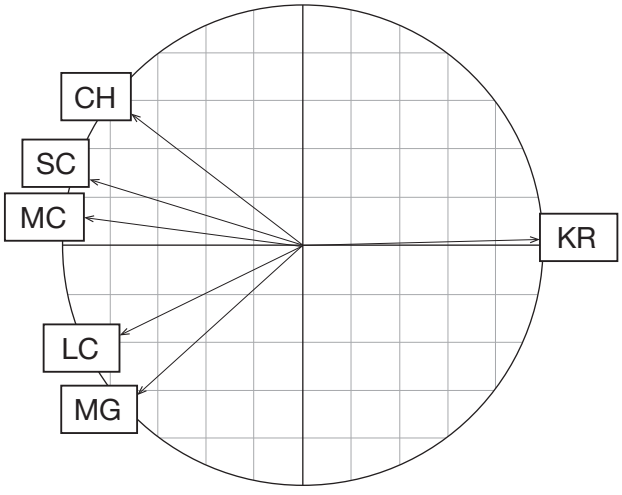


Fig. 12. Principal component analysis correlation (PCA) circle on axes 1 and 2. KR: krill; CH: chaetognaths; SC: small copepods; MC: small to medium copepods; MG: medium to large copepods; LC: large copepods

on an ADCP is designed to amplify echo intensity to a fixed level when the signal to noise ratio decreases in depth and the spectrum becomes more flat, $k_c$ may become depth dependent. We only applied the calibration relationship in Wilhelmina Bay where the ADCP and EK-60 calibrations occurred because this calibration approach is purely empirical and cannot generally be applied to other studies.

By using the total biomass estimates (in WW) from MOCNESS samples (Table 2) and ADCP backscattering (Fig. 7) and assuming the mean length of 42 mm, the maximum abundance estimates of krill were $1.6 \times 10^4$ and $4.5 \times 10^4$ ind. $m^{-2}$ at Stn B for each method, respectively. The krill biomass estimate based on MOCNESS samples is 3 times lower than that estimated from ADCP backscattering. Such differences have been found in a number of acoustic studies to be caused by the variability of length–target strength conversion, size distributions, varied acoustic properties, and net avoidance by organisms (Chu et al. 1993, Zhou et al. 1994, Demer & Hewitt 1995, Demer & Martin 1995, Lawson et al. 2004). The use of strobe lights can significantly improve the krill catch efficiency of a net tow by reducing net avoidance, which improves cross-correlations between net and acoustic krill abundance and biomass estimates (Wiebe et al. 2004). It is also possible that low sampling effort of net tows missed the highest abundances of krill near Stn B.

The high abundance of krill in the inner part of Wilhelmina Bay may be associated with the anticyclonic circulation over the deep basin and intrusion of warm waters at the depth from the Gerlache Strait (Figs. 4 & 7). If krill stayed at 150 to 300 m depth during the day, they would be transported into the inner bay by the deep current; when krill are distributed near the surface during the night, they would be retained by the anticyclonic circulation or transported out the bay by surface wind driven currents. However, krill were actively aggregating in the inner bay against currents.

### Changes in biomass and abundance of different trophic levels

The phytoplankton concentration decreased from ~2.3 g C $m^{-2}$ during Leg 1 to 1.1 g C $m^{-2}$ during Leg 2, and to 0.7 g C $m^{-2}$ during Leg 3 at Stn A (Table 2). Though these values were not calibrated and can only be treated as relative values, they showed the monotonic temporal decrease in phytoplankton biomass during the fall to winter transition period. The ratio of phytoplankton to krill biomass based on MOCNESS samples varied by ~3 to 10 % at Stn A and 0.3 % at Stn B. If using the krill biomass estimates based on the ADCP, which were 3 times higher than that of MOCNESS samples, these ratios would be 1 to 3 % at Stn A and 0.1 % at Stn B.

The copepod biomass for Legs 1, 2 and 3 was 0.21, 0.36 and 0.41 g C $m^{-2}$ at Stn A, respectively, and was 0.54, 0.69 and 1.5 g C $m^{-2}$ at Stn B, respectively. This successive increase in biomass from Leg 1 to Leg 3 at both stations was primarily caused by a rapid increase of abundance in medium to large copepods dominated by *Metridia gerlachei* in deep waters. At this relatively low phytoplankton biomass period, the copepod biomass increase is unlikely to have been the result of population growth. Alternatively, the increase in *M. gerlachei* in deep waters could be

advected along the observed deep inward current from the Gerlache Strait.

The krill aggregations sampled during May 2009 in Wilhelmina Bay covered a surface area of ~10 × 10 km², leading to a super-aggregation of krill and whales (Nowacek et al. 2011). At both Stn A outside of the aggregation and Stn B within the aggregation, adult krill dominated biomass estimates in the water column. During the cruise, the krill biomass at Stn B decreased 4 times over the 28 d while the krill biomass at Stn A remained very low but steady. Based on the MOCNESS tow samples, the decrease in biomass at Stn B from ~800 g C $m^{-2}$ on Day 0 to 340 and 210 g C $m^{-2}$ on Days 16 and 28, respectively, (Tables 1 & 2) was equivalent to a specific population change rate of –0.048 $d^{-1}$, as determined by using the standard mortality rate definition (Harris et al. 2000, Zhou et al. 2004). Though there were only 3 samples, the trend was significant. This rate includes mortality and gain or loss in abundance due to dispersion fluxes at the boundaries. *In situ* mortality of krill has been rarely estimated because of a lack of methods in general for zooplankton (Aksnes et al. 1997). In a field study on euphausiids in a subarctic fjord, the mortality was found to be ~0.23 $d^{-1}$, which was the result of heavy feeding by dense populations of cod and herring (Edvardsen et al. 2002). In Wilhelmina Bay, the mortality for krill was much lower than that determined by Edvardsen et al. (2002). The estimated daily consumption of ~306 whales in Wilhelmina Bay during our 34 d study was between 0.16 and 0.36% of krill biomass, equivalent to a predation mortality rate of less than 0.01 $d^{-1}$, which was considered negligible to the available krill abundance (Nowacek et al. 2011). Thus, the starvation mortality rate was probably higher than the predation mortality rate.

### Changes in zooplankton vertical distributions

The small copepod group primarily consisted of the cyclopoid copepods *Oithona* spp. and *Oncaea* spp., and the calanoid species *Microcalanus pygmaeus*. The biomass of small copepods changed from 5.7% of total zooplankton biomass at Stn A to 1.6% at Stn B (Table 3). The medium to large copepods, primarily dominated by *Metridia gerlachei*, had the greatest biomass within the zooplankton community. In Wilhelmina Bay, *M. gerlachei* were vertically distributed between 89 and 151 m at Stn A, and between 271 and 334 m at Stn B. The vertical distributions of small, small to medium and medium to large copepods had maximum densities at the surface for Stn A with the exception of Leg 1. Within krill aggregations at Stn B, the vertical distributions of small, small to medium and medium to large copepods had density minima at the surface, which was occupied by krill aggregations. During the night, a sharp increase in copepod abundance occurred at the vertical edge of krill aggregations. The adult or older copepodite stages of 4 calanoid species constituted the group of large copepods and included *Calanus acutus, C. propinquus*, *Euchaeta antarctica* and *Rhincalanus gigas*. Except for *E. antarctica*, these species are herbivorous and undergo a vertical seasonal migration into deep waters after mid fall (Marin & Schnack-Schiel 1993, Zmijewska & Yen 1993, Schnack-Schiel & Hagen 1994, Atkinson 1998). We found this copepod size group most abundant in deeper waters, as expected, although some tows caught large copepods in the surface layers. *E. antarctica* is a carnivorous copepod and were found throughout the entire water column, which was similar to previous observations (Hopkins 1985).

Chaetognaths, primarily *Eukrohnia hamata*, contributed 32 and 16% of the total zooplankton biomass at Stns A and B, respectively. The total chaetognath biomass found in Wilhelmina Bay was consistent with that of other studies done in the Gerlache Strait (Øresland 1995). Chaetognaths prey on copepods and other zooplankton. They primarily stayed in waters deeper than 150 m at both Stns A and B independent of krill aggregations and coincident with high concentrations of zooplankton biomass.

### Interaction between krill and copepods

Our observations showed that the small and the medium to large copepods were abundant in the upper 150 m during Legs 2 and 3 in the absence of krill aggregations at Stn A, but they were absent in dense krill aggregations at Stn B (Table 2, Fig. 10). The surface currents in Wilhelmina Bay formed an anticyclonic gyre with speeds of ~10 to 20 cm $s^{-1}$, which would transport and disperse zooplankton uniformly throughout the bay. Thus, the low abundance of copepods at Stn B could reasonably be explained by predation mortality, competitive exclusion or both. Among copepod predators, chaetognaths remained below 150 m and could probably not contribute to the disappearance of copepods in the upper 150 m. *Euphausia superba* were the most abundant micronekton in the upper layer at night, and feed and co-occur with the decreased

abundance of small and medium to large copepods (Fig. 11).

The medium to large copepods, mainly *Metridia gerlachei*, were primarily in the upper 150 m and few were in the deep water at Stn A. Conversely, few were in the upper 150 m within the krill layer while *M. gerlachei* were abundant deeper than 200 m at Stn B (Fig. 11). *M. gerlachei* is primarily herbivorous (Zmijewska & Yen 1993, Schnack-Schiel & Hagen 1994, Lopez & Huntley 1995). They were at the surface to feed on the low concentration of available phytoplankton at Stn A. Because the water properties and phytoplankton levels at both stations were quite similar, decreased abundance of *M. gerlachei* at Stn B was most probably due to either being preyed upon or excluded by the dense *Euphausia superba* aggregations. Since *M. gerlachei* are strong swimmers and capable of migrating vertically (Lopez & Huntley 1995), they may have stayed in deep waters and avoided krill aggregations during the night.

### Krill grazing and energetics

Our study period in the mid fall coincided with the transition period of krill prey fields, which is due to the decrease in the amount of daylight (Price et al. 1988, Hopkins et al. 1993, Atkinson & Snÿder 1997, Zhou et al. 2004). This decrease causes a rapid decrease in phytoplankton from 1.5 to 0.25 mg $m^{-3}$ at the surface, and krill may have to switch to an omnivorous diet, which delays development, reduces metabolism or uses stored lipids. Estimates of krill-specific carbon daily ration from both laboratory and *in situ* measurements are ~0.1 to 0.5% of their body biomass in winter under reduced metabolism (Atkinson et al. 2002) and 1 to 10% in other seasons (Ikeda 1981, Huntley et al. 1994, Atkinson & Snÿder 1997, Perissinotto et al. 1997, Meyer et al. 2010). During our cruise, krill vertically migrated between day and night probably due to feeding activities and predator avoidance (Fig. 8). However, the total standing stock of phytoplankton based on fluorescence measurements was ~0.3% of krill biomass at Stn B. Based on acoustic estimates, which were 3 times greater than that of net tows, the phytoplankton biomass was only 0.1% of the krill biomass. Though the fluorometer was not calibrated *in situ*, the measured phytoplankton concentrations were very low and probably contributed little to the krill diet. If krill had fed non-selectively, they should have stayed in deep waters where the zooplankton biomass was more than the phytoplankton biomass at the surface. However, krill aggregations exhibited diel vertical migrations throughout our study period even though phytoplankton monotonically decreased in the upper layer, which provided a small percentage of the food needed by krill; zooplankton in deeper waters may be another food source for krill (Table 5, Figs. 8 & 11). Thus, their persistent surface feeding suggests that phytoplankton, even at very low concentrations, were still the preferred food for krill.

The krill aggregation found in Wilhelmina Bay was larger than any reported in the past 20 yr (Atkinson et al. 2008, Nowacek et al. 2011). The conservative estimate of mean biomass concentration from MOCNESS tows reached 200 to 800 g C $m^{-2}$. Based on these values and assuming 1 to 10% of biomass as the daily metabolic rate of an active krill during summer, the mean krill concentration would require a daily consumption rate of 2 to 80 g C $m^{-2}$ $d^{-1}$. The upper end of this daily consumption within such a super-aggregation is not realistic compared with the upper end of the summer primary production estimated to range from 1.4 to 12.5 g C $m^{-2}$ $d^{-1}$ near Palmer Station (Moline & Prézelin 1996, Garibotti et al. 2005, Ducklow et al. 2007). The formation, maintenance and fate of this super-aggregation of krill at such a scale remain unanswered.

Previous studies indicate that *Euphausia superba* is able to feed on a wide size range of prey including large copepods (Price et al. 1988, Atkinson & Snÿder 1997). From our statistical analyses, it is most likely that krill were feeding on the small and small to medium copepods. Atkinson & Snÿder (1997) found *E. superba* feed preferentially on small calanoids (<3 mm) that provide high concentrations of food, although no research has examined this in the natural environment. At Stn B, the biomasses of small and small to medium size copepods below 150 m in Leg 3 were 2 to 3 times more than that of Leg 1. In late fall, when primary production is limited by light and deep mixing, the abundances and biomass of zooplankton

Table 5. Biomass ratios of copepods (see Table 3 for size categories) and phytoplankton to krill at Stn B based on live samples collected during 3 legs using the MOCNESS

| Group | Percentage (%) of krill carbon biomass | | |
|---|---|---|---|
| | Leg 1 | Leg 2 | Leg 3 |
| Copepods | 0.06 | 0.19 | 0.72 |
| Small and small to medium copepods | 0.01 | 0.03 | 0.15 |
| Phytoplankton | 0.32 | 0.29 | 0.35 |

decrease (Atkinson 1998, Ashjian et al. 2004, Zhou et al. 2004). Thus, the increases in small and small to medium copepods in the inner Wilhelmina Bay had to be supplied from sources outside of the bay by the advection in deep waters between Leg 1 and Leg 3 (Table 5). The available biomass estimates of small and small to medium copepods were only about 0.01, 0.03 and 0.15% of krill carbon biomass for Legs 1, 2 and 3, respectively. Though small to medium mesozooplankton contributed to the diet of the krill aggregation, it is unlikely that available concentrations could meet the food demand of these krill.

The biomass percentages of total phytoplankton and copepods to krill biomass at Stn B were 0.38, 0.48 and 1.07% in Legs 1, 2 and 3, respectively (Table 5). The increase in the percentage reflects both the decrease in krill biomass and monotonic increase in mesozooplankton biomass. The whale predation mortality rate was less than 0.01 $d^{-1}$ and interpreted as negligible (Nowacek et al. 2011). The decrease in krill biomass could be caused by current advection out of the bay, active swimming out of the bay, starvation mortality or predation by other top predators. When the mesozooplankton biomass was continuously maintained by advection of the deep intruding current, as evidenced by the increase in mesozooplankton biomass in response to the decrease in krill biomass due to mortality or migration, the ratio of total phytoplankton and zooplankton biomass to krill changed from 0.38% in Leg 1 to 1.07% in Leg 3, reaching the lower limit of krill daily ration (Ikeda 1981, Huntley et al. 1994, Atkinson & Snÿder 1997, Perissinotto et al. 1997, Meyer et al. 2010). Krill can feed on zooplankton and use this as an overwintering strategy if zooplankton can be sufficiently supplied by deep current advection and upwelling throughout the winter.

Our observations suggest that krill had to feed omnivorously (i.e. on phytoplankton as well as small and small to medium zooplankton) during the austral fall, which is consistent with overwintering strategies determined from previous observations from laboratory experiments (Price et al. 1988, Atkinson & Snÿder 1997). Our data provide *in situ* evidence on distributions of krill and mesozooplankton that elucidates possible prey–predator interactions at a scale of the super-aggregation. At this spatial scale, both primary production and transport of mesozooplankton would not supply enough food for this krill aggregation, and the size of this aggregation would be reduced to an unknown level through the winter. We speculate that large amounts of biota associated with spring and fall blooms are trapped in the Gerlache Strait and embayments and include high densities of zooplankton and detritus, which may attract krill to aggregate in these embayments. However, such a scale of aggregation may cause severe mortality in krill due to starvation, and attraction and concentration of top predators such as whales, seals and birds may intensify their interactions with the krill. Understanding the mechanisms and the timing of these aggregations and evolution of food web structures is critical to improve our knowledge and management of the Antarctic ecosystem.

*Acknowledgements.* We thank the Captain and crews of the ASRV 'LM Gould' and Raytheon Polar Service Company for all their assistance during the cruise. We acknowledge E. Firing and J. Hummon at the University of Hawaii and T. Chereskin at Scripps Institution of Oceanography for the ADCP operation and data acquisition during the cruise. This research was supported by the US National Science Foundation grants ANT-0739566 and ANT-073948. B.E. acknowledges the PhD fellowship from CNRS.

## LITERATURE CITED

Aksnes DL, Miller CB, Ohman MD, Wood SN (1997) Estimation techniques used in studies of copepod population dynamics — a review of underlying assumptions. Sarsia 82:279–296

Ashjian CJ, Rosenwaks GA, Wiebe PH, Davis CS and others (2004) Distribution of zooplankton on the continental shelf off Marguerite Bay, Antarctic Peninsula, during austral fall and winter, 2001. Deep-Sea Res II 51: 2073–2098

Atkinson A (1998) Life cycle strategies of epipelagic copepods in the Southern Ocean. J Mar Syst 15:289–311

Atkinson A, Snÿder R (1997) Krill–copepod interactions at South Georgia, Antarctica, I. Omnivory by *Euphausia superba.* Mar Ecol Prog Ser 160:63–76

Atkinson A, Meyer B, Stübing D, Hagen W, Bathmann UV (2002) Feeding and energy budgets of Antarctic krill *Euphausia superba* at the onset of winter. II. Juveniles and adults. Limnol Oceanogr 47:953–966

Atkinson A, Siegel V, Pakhomov EA, Rothery P and others (2008) Oceanic circumpolar habitats of Antarctic krill. Mar Ecol Prog Ser 362:1–23

Beardsley RC, Limeburner R, Brechner Owens W (2004) Drifter measurements of surface currents near Marguerite Bay on the western Antarctic Peninsula shelf during austral summer and fall, 2001 and 2002. Deep-Sea Res II 51:1947–1964

Breiman L (2001) Random forests. Mach Learn 45:5–32

Bretherton FP, Davis RE, Fandry CB (1976) A technique for objective analysis and design of oceanographic experiments applied to MODE-73. Deep-Sea Res 23:559–582

Brierley AS, Brandon MA, Watkins JL (1998) An assessment of the utility of an acoustic Doppler current profiler for biomass estimation. Deep-Sea Res I 45:1555–1573

Chu D, Wiebe PH (2005) Measurements of sound-speed and density contrasts of zooplankton in Antarctic waters. ICES J Mar Sci 62:818–831

Chu D, Foote KG, Stanton TK (1993) Further analysis of target strength measurements of Antarctic krill at 38 and 120 kHz: comparison with deformed cylinder model and inference of orientation distribution. J Acoust Soc Am 93: 2985–2988

Daly KL (2004) Overwintering growth and development of larval *Euphausia superba*: an interannual comparison under varying environmental conditions west of the Antarctic Peninsula. Deep-Sea Res II 51:2139–2168

Daly KL, Macaulay MC (1988) Abundance and distribution of krill in the ice edge zone of the Weddell Sea, austral spring 1983. Deep-Sea Res A 35:21–41

Demer DA, Hewitt RP (1995) Bias in acoustic biomass estimates of *Euphausia superba* due to diel vertical migration. Deep-Sea Res I 42:455–475

Demer DA, Martin LV (1995) Zooplankton target strength: volumetric or areal dependence? J Acoust Soc Am 98: 1111–1118

Dorland RD, Zhou M (2008) Circulation and heat fluxes during the austral fall in George VI Sound, Antarctic Peninsula. Deep-Sea Res II 55:294–308

Ducklow HW, Baker K, Martinson DG, Quetin LB and others (2007) Marine pelagic ecosystems: the West Antarctic Peninsula. Philos Trans R Soc B 362:67–94

Edvardsen A, Zhou M, Tande KS, Zhu Y (2002) Zooplankton population dynamics: measuring *in situ* growth and mortality rates using an Optical Plankton Counter. Mar Ecol Prog Ser 227:205–219

El-Sayed SZ (1996) Historical perspective of research in the Antarctic Peninsula region. Antarct Res Ser 70:1–13

Everson I (2000) Distribution and standing stock: the Southern Ocean. In: Everson I (ed) Krill biology, ecology and fisheries. Blackwell, Cambridge, p 63–79

Flagg CN, Smith SL (1989) On the use of the acoustic Doppler current profiler to measure zooplankton abundance. Deep-Sea Res 36:455–474

Foote KG, Everson I, Watkins JL, Bone DG (1990) Target strengths of Antarctic krill (*Euphausia superba*) at 38 and 120 kHz. J Acoust Soc Am 87:16–24

Friedlaender AS, Halpin PN, Qian SS, Lawson G, Wiebe P, Thiele D, Read AJ (2006) Whale distribution in relation to prey abundance and oceanographic processes in shelf waters of the Western Antarctic Peninsula. Mar Ecol Prog Ser 317:297–310

Garibotti IA, Vernet M, Ferrario ME, Smith RC, Ross RM, Quetin LB (2003) Phytoplankton spatial distribution patterns along the western Antarctic Peninsula (Southern Ocean). Mar Ecol Prog Ser 261:21–39

Garibotti IA, Vernet M, Smith RC, Ferrario ME (2005) Interannual variability in the distribution of the phytoplankton standing stock across the seasonal sea-ice zone west of the Antarctic Peninsula. J Plankton Res 27:825–847

Gasparini S (2007) PLANKTON IDENTIFIER: a software for automatic recognition of planktonic organisms. www.obs-vlfr.fr/~gaspari/Plankton_Identifier/index.php

Grosjean P, Picheral M, Warembourg C, Gorsky G (2004) Enumeration, measurement, and identification of net zooplankton samples using the ZOOSCAN digital imaging system. ICES J Mar Sci 61:518–525

Hagen W, Van Vleet ES, Kattner G (1996) Seasonal lipid storage as overwintering strategy of Antarctic krill. Mar Ecol Prog Ser 134:85–89

Hamner WM (1984) Aspects of schooling in *Euphausia superba*. J Crustac Biol 4(Spec 1):67–74

Harris RP, Wiebe PH, Lenz J, Skjoldal HR, Huntley M (2000) ICES zooplankton methodology manual. Academic Press, London

Hofmann EE, Klinck JM, Loscarnini RA, Fach BA, Murphy EJ (1988) Krill transport in the Scotia Sea and environs. Antarct Sci 10:210–231

Hofmann EE, Klinck JM, Lascara CM, Smith DA (1996) Water mass distribution and circulation west of the Antarctic Peninsula and including Bransfield strait. In: Ross RM, Hofmann EE, Quetin LB (eds) Foundations for ecological research west of the Antarctic Peninsula. Antarct Res Ser 70:61–80

Hofmann EE, Klinck JM, Costa DP, Daly KL, Torres JJ, Fraser W (2002) US Southern Ocean global ocean ecosystems dynamics program. Oceanography 15:64–74

Hopkins TL (1985) The zooplankton community of Croker Passage, Antarctic Peninsula. Polar Biol 4:161–170

Hopkins TL, Lancraft TM, Torres JJ, Donnelly J (1993) Community structure and trophic ecology of zooplankton in the Scotia Sea marginal ice zone in winter (1988). Deep-Sea Res I 40:81–105

Huntley ME, Nordhausen W, Lopez MDG (1994) Elemental composition, metabolic activity and growth of Antarctic krill *Euphausia superba* during winter. Mar Ecol Prog Ser 107:23–40

Ikeda T (1981) Metabolic activity of larval stages of Antarctic krill. Antarct J US 16:161–162

Ikeda T, Dixon P (1982) Body shrinkage as a possible overwintering mechanism of the Antarctic krill, *Euphausia superba* Dana. J Exp Mar Biol Ecol 62:143–151

Klinck JM, Hofmann EE, Beardsley RC, Salihoglu B, Howard S (2004) Water-mass properties and circulation on the west Antarctic Peninsula continental shelf in austral fall and winter 2001. Deep-Sea Res II 51:1925–1946

Lascara CM, Hofmann EE, Ross RM, Quetin LB (1999) Seasonal variability in the distribution of Antarctic krill, *Euphausia superba*, west of the Antarctic Peninsula. Deep-Sea Res I 46:951–984

Laws R (1985) The ecology of the Southern Ocean. Am Sci 73:26–40

Lawson GL, Wiebe PH, Ashjian CJ, Gallager SM, Davis CS, Warren JD (2004) Acoustically-inferred zooplankton distribution in relation to hydrography west of the Antarctic Peninsula. Deep-Sea Res II 51:2041–2072

Lawson GL, Wiebe PH, Ashjian CJ, Chu D, Stanton TK (2006) Improved parametrization of Antarctic krill target strength models. J Acoust Soc Am 119:232–242

Loeb V, Siegel V, Holm-Hansen O, Hewitt R, Fraser W, Trivelpiece W, Trivelpiece S (1997) Effects of sea-ice extent and krill or salp dominance on the Antarctic food web. Nature 387:897–900

Lopez MDG, Huntley ME (1995) Feeding and diel vertical migration cycles of *Metridia gerlachei* (Giesbrecht) in coastal waters of the Antarctic Peninsula. Polar Biol 15: 21–30

Marin VH, Schnack-Schiel SB (1993) The occurrence of *Rhincalanus gigas, Calanoides acutus*, and *Calanus propinquus* (Copepoda: Calanoida) in late May in the area of the Antarctic Peninsula. Polar Biol 13:35–40

Marr JWS (1962) The natural history and geography of the Antarctic krill (*Euphausia superba* Dana). Discovery Rep 32:33–464

Marschall HP (1988) The overwintering strategy of Antarctic krill under the pack-ice of the Weddell Sea. Polar Biol 9: 129–135

Meyer B, Auerswald L, Siegel V, Spahi S and others (2010)

Seasonal variation in body composition, metabolic activity, feeding, and growth of adult krill *Euphausia superba* in the Lazarev Sea. Mar Ecol Prog Ser 398:1–18

Mitchell BG, Holm-Hansen O (1991) Observations and modeling of the Antarctic phytoplankton crop in relation to mixing depth. Deep-Sea Res 38:981–1007

Moline MA, Prézelin BB (1996) Long-term monitoring and analyses of physical factors regulating variability in coastal Antarctic phytoplankton biomass, *in situ* productivity and taxonomic composition over subseasonal, seasonal and interannual time scales phytoplankton dynamics. Mar Ecol Prog Ser 145:143–160

Nicol S (2003) Living krill, zooplankton and experimental investigations: a discourse on the role of krill and their experimental study in marine ecology. Mar Freshwat Behav Physiol 36:191–205

Niiler PP, Amos AF, Hu JH (1991) Water masses and 200 m relative geostrophic circulation in the western Bransfield Strait region. Deep-Sea Res II 38:943–959

Nowacek DP, Friedlaender AS, Halpin PN, Hazen EL and others (2011) Super-aggregations of krill and humpback whales in Wilhelmina Bay, Antarctic Peninsula. PLoS ONE:e19173

Øresland V (1995) Winter population structure and feeding of the chaetognath *Eukrohnia hamata* and the copepod *Euchaeta antarctica* in Gerlache Strait, Antarctic Peninsula. Mar Ecol Prog Ser 119:77–86

Padman P, Fricker HA, Coleman R, Howard S, Erofeeva L (2002) A new tide model for the Antarctic ice shelves and seas. Ann Glaciol 34:247–254

Pedlosky J (1987) Geophysical fluid dynamics. Springer-Verlag, New York, NY

Perissinotto R, Pakhomov EA, McQuaid CD, Froneman PW (1997) *In situ* grazing rates and daily ration of Antarctic krill *Euphausia superba* feeding on phytoplankton at the Antarctic Polar Front and the Marginal Ice Zone. Mar Ecol Prog Ser 160:77–91

Price HJ, Boyd KR, Boyd CM (1988) Omnivorous feeding behavior of the Antarctic krill *Euphausia superba.* Mar Biol 97:67–77

Quetin LB, Ross RM (1991) Behavioural and physiological characteristics of the Antarctic krill, *Euphausia superba.* Am Zool 31:49–63

Quetin LB, Ross RM, Clarke A (1994) Krill energetics: seasonal and environmental aspects of the physiology of *Euphausia superba.* In: El-Sayed SZ (ed) Southern Ocean ecology: the BIOMASS perspective. Cambridge University Press, Cambridge, p 165–184

Rakotomalala R (2005) TANAGRA: un logiciel gratuit pour l'enseignement et la recherche. In: Actes de EGC 2005, RNTI-E-3 2:697–702

Rasband WS (2005) ImageJ. US National Institutes of Health, Bethesda, MD. http://rsbweb.nih.gov/ij

RDI (RD Instruments) (1989) Acoustic Doppler current profilers principles of operation: a practical primer. RDI, San Diego, CA

Rodriguez J, Jiménez-Gómez F, Blanco JM, Figueroa FL (2002) Physical gradients and spatial variability of the size structure and composition of phytoplankton in the Gerlache Strait (Antarctica). Deep-Sea Res II 49:693–706

Ross RM, Quetin LB (2000) Reproduction in euphausiids. In: Everson I (ed) Krill: biology, ecology, and fisheries. Blackwell Science, Oxford, p 150–181

Schnack-Schiel SB, Hagen W (1994) Life cycle strategies and seasonal variations in distribution and population structure of four dominant calanoid copepod species in the eastern Weddell Sea, Antarctica. J Plankton Res 16: 1543–1566

Siegel V (2005) Distribution and population dynamics of *Euphausia superba*: summary of recent findings. Polar Biol 29:1–22

Siegel V, Kalinowski J (1994) Krill demography and small-scale processes: a review. In: El-Sayed SZ (ed) Southern Ocean ecology: the BIOMASS perspective. Cambridge University Press, New York, NY, p 145–163

Smith DA, Hofmann EE, Klinck JM, Lascara CM (1999) Hydrography and circulation of the west Antarctic Peninsula continental shelf. Deep-Sea Res I 46:925–949

Tarling GA, Shreeve RS, Hirst AG, Atkinson A, Pond DW, Murphy EJ, Watkins JL (2006) Natural growth rates in Antarctic krill (*Euphausia superba*): I. Improving methodology and predicting intermolt period. Limnol Oceanogr 51:959–972

Thiele D, Chester ET, Moore SE, Sirovic A, Hildebrand JA, Friedlaender AS (2004) Seasonal variability in whale encounters in the western Antarctic Peninsula. Deep-Sea Res II 51:2311–2325

Torres JJ, Donnelly J, Hopkins TL, Lancraft TM, Aarset AV, Ainley DG (1994) Proximate composition and overwintering strategies of Antarctic micronektonic Crustacea. Mar Ecol Prog Ser 113:221–232

Wiebe PH, Boyd S, Cox JL (1975) Relationships between zooplankton displacement volume, wet weight, dry weight, and carbon. Fish Bull 73:777–786

Wiebe P, Burt KH, Boyd SH, Morton AW (1976) A multiple opening/closing net and environmental sensing system for sampling zooplankton. J Mar Res 34:341–354

Wiebe PH, Morton AW, Bradley AM, Backus RH and others (1985) New development in the MOCNESS, an apparatus for sampling zooplankton and micronekton. Mar Biol 87:313–323

Wiebe P, Ashjian C, Gallager S, Davis C, Lawson G, Copley N (2004) Using a high-powered strobe light to increase the catch of Antarctic krill. Mar Biol 144:493–502

Zhou M, Dorland RD (2004) Aggregation and vertical migration behavior of *Euphausia superba.* Deep-Sea Res II 51: 2119–2137

Zhou M, Huntley ME (1996) The principle of biological attraction, demonstrated by the bio-continuum theory of zooplankton patch dynamics. J Mar Res 54:1017–1037

Zhou M, Nordhausen W, Huntley M (1994) ADCP measurements of the distribution and abundance of euphausiids near the Antarctic Peninsula in winter. Deep-Sea Res I 41:1425–1445

Zhou M, Niiler PP, Hu JH (2002) Surface currents in the Bransfield and Gerlache Straits, Antarctica. Deep-Sea Res I 49:267–280

Zhou M, Zhu Y, Peterson JO (2004) *In situ* growth and mortality of mesozooplankton during the austral fall and winter in Marguerite Bay and its vicinity. Deep-Sea Res II 51:2099–2118

Zhou M, Niiler PP, Zhu Y, Dorland RD (2006) The western boundary current in the Bransfield Strait, Antarctica. Deep-Sea Res I 53:1244–1252

Zmijewska MI, Yen J (1993) Seasonal and diel changes in the abundance and vertical distribution of the Antarctic copepod species *Calanoides acutus*, *Calanus propinquus*, *Rhincalanus gigas*, *Metridia gerlachei* and *Euchaeta antarctica* (Calanoida) in Croker Passage (Antarctic Peninsula). Oceanologia 35:101–127

*Editorial responsibility: Matthias Seaman, Oldendorf/Luhe, Germany*

*Submitted: June 17, 2011; Accepted: January 26, 2012*
*Proofs received from author(s): April 9, 2012*